

A New Approach to Obtain Limited Diffraction Beams

Jian-yu Lu, *Member, IEEE*, Hehong Zou, and James F. Greenleaf, *Fellow, IEEE*

Abstract—Limited diffraction beams were first discovered by Durnin in 1987 (formerly named nondiffracting or diffraction-free beams by Durnin). Since then, new families of limited diffraction beams have been discovered. Theoretically, limited diffraction beams can propagate to infinite distance without diffracting or spreading. Even if they are produced with a finite aperture radiator, limited diffraction beams have a large depth of field. Because of this property, limited diffraction beams could have applications in medical imaging, tissue characterization, and nondestructive evaluation, as well as other wave related areas such as electromagnetics and optics. In this paper, we develop a novel approach that can convert any diffracting solution of the isotropic-homogeneous wave equation to a limited diffraction solution. As an example, this approach was applied to an n -dimensional wavelet solution that we generalized from the three-dimensional solution obtained by Kaiser *et al.* This example establishes a relationship between localized limited diffraction beams and the wavelet theory. The resulting limited diffraction beam was compared with those discovered previously.

I. INTRODUCTION

IN 1983, Brittingham discovered the first localized waves that he termed “focus wave modes” [1]. The localized waves can propagate to a large distance with only local deformation. These waves were further developed and studied by Ziolkowski [2] and many other investigators [3]–[11]. The first limited diffraction beam was found in 1987 by Durnin [12], [13] (to avoid the controversy of Durnin’s original terminologies “nondiffracting beams” and “diffraction-free beams,” we used the term “limited diffraction beams” [14]). Unlike localized waves, limited diffraction beams in theory do not deform as they propagate to infinite distance while maintaining a high localization. Recently, a new family of limited diffraction beams (termed X-waves because of their X-like shape in a plane along the wave axis) was discovered [15], [16]. The new waves do not spread even for a large bandwidth. When produced with a finite aperture radiator, limited diffraction beams have a large depth of field (constant high resolution over a large distance). Because of this property, limited diffraction beams could have applications in medical imaging [17]–[19], tissue characterization [20], nondestructive evaluation [21], and Doppler blood flow estimation [22].

Manuscript received November 22, 1993; revised April 10, 1995. This work was supported in part by Grants CA 54212 and CA 43920 from the National Institutes of Health.

J. Lu and J. F. Greenleaf are with the Biodynamics Research Unit, Department of Physiology and Biophysics, Mayo Clinic and Foundation, Rochester, MN 55905 USA.

H. Zou is with Rosemount Inc., Chanhassen, MN USA.
IEEE Log Number 9413777.

In this paper we developed a novel approach that can convert any diffracting solution of the isotropic-homogeneous (or free-space) scalar wave equation to a limited diffraction solution [15], [23]. As an example, this method was applied to an n -dimensional solution that we generalized from a 3-D localized spherical wavelet solution developed by Kaiser *et al.* [24]–[26]. This establishes the relationship between limited diffraction beams and wavelet waves (wavelet theory). In addition, the new limited diffraction beam obtained with this method was compared to those discovered previously [14], [15], [23].

II. THEORY

In this section, we will develop a novel approach that can convert any diffracting solution of the isotropic-homogeneous wave equation to a limited diffraction solution.

The n -dimensional isotropic-homogeneous scalar wave equation is given by

$$\left[\sum_{j=1}^n \frac{\partial^2}{\partial x_j^2} - \frac{1}{c^2} \frac{\partial^2}{\partial t^2} \right] \Phi_n(x_1, x_2, \dots, x_n, t) = 0, \quad (1)$$

where $\Phi_n(x_1, x_2, \dots, x_n, t)$ denotes the acoustic pressure at the n -dimensional point $\vec{r} = (x_1, x_2, \dots, x_n)$ and time t , x_j are spatial variables in rectangular coordinates, c is the speed of sound in the medium and $n \geq 1$ is an integer.

To obtain a wave (or beam) that will propagate along one of the spatial axes, say, x_n , with time t and does not spread when propagating, we will seek a solution such that $x_n - c_1 t$ appears as a single term like the equations derived in [15], [23], where c_1 is a constant related to the speed of sound c . With this specific task in mind, we first consider the $(n-1)$ -dimensional wave equation (let $n \rightarrow n-1$ in (1))

$$\left[\sum_{j=1}^{n-1} \frac{\partial^2}{\partial x_j^2} - \frac{1}{c^2} \frac{\partial^2}{\partial t^2} \right] \Phi_{n-1}(\vec{r}, t) = 0, \quad (2)$$

where $\Phi_{n-1}(\vec{r}, t)$ denotes the wave field in the $(n-1)$ -dimensional space $\vec{r} = (x_1, x_2, \dots, x_{n-1})$ and at time t .

It is easy to verify that if $\Phi_{n-1}(\vec{r}, t)$ is a solution to (2), it will be a limited diffraction solution to (1) after the following variable substitution

$$\vec{r} \sin \zeta \rightarrow \vec{r}, \quad \text{and} \quad \frac{x_n \cos \zeta}{c} - t \rightarrow t, \quad (3)$$

where $0 < \zeta < \pi$ is a real constant. Using the substitution in (3), from (2) we have

$$\left[\sum_{j=1}^{n-1} \frac{\partial^2}{\partial x_j^2} \right] \Phi_{n-1} \left(\vec{r} \sin \zeta, \frac{x_n \cos \zeta}{c} - t \right) = (\sin \zeta)^2 \frac{1}{c^2} \frac{\partial^2}{\partial t^2} \Phi_{n-1} \left(\vec{r} \sin \zeta, \frac{x_n \cos \zeta}{c} - t \right), \quad (4)$$

and

$$\frac{\partial^2}{\partial x_n^2} \Phi_{n-1} \left(\vec{r} \sin \zeta, \frac{x_n \cos \zeta}{c} - t \right) = (\cos \zeta)^2 \frac{1}{c^2} \frac{\partial^2}{\partial t^2} \Phi_{n-1} \left(\vec{r} \sin \zeta, \frac{x_n \cos \zeta}{c} - t \right). \quad (5)$$

Summing both the left- and right-hand sides of (4) and (5), and comparing the results with (1), we see that

$$\Phi_{n-1}(\vec{r} \sin \zeta, x_n \cos \zeta / c - t) \quad (6)$$

is a solution to (1). In addition, because the variables, x_n and t , appear in the form, $x_n \cos \zeta / c - t$, (6) represents a limited diffraction beam. In other words, if $x_n \cos \zeta / c - t = \text{constant}$ (travels with the wave at the speed, $c / \cos \zeta$, along the axis, x_n), (6) is not a function of x_n and t (an unchanged wave package).

Notice that the above conversion to a limited diffraction beam is valid only when $n - 1 \geq 1$ in (2). For $n - 1 = 0$, $\Phi_{n-1}(\vec{r}, t) = \Phi_0(t)$ represents a vibration, not a wave. In this case, $\Phi_0(t)$ can only be converted to a limited diffraction wave when $\cos \zeta = 1$ in (3). In addition, the “-” sign in (3) can be changed to “+,” which represents a wave going along $-x_n$ direction.

III. APPLICATION TO WAVELET SOLUTION

The method developed in the last section can be applied to an arbitrary solution of (1). However, we are particularly interested in those solutions which have some kind of localization. The wavelet solution [24]–[26] developed with the wavelet theory is localized and we will use it as an example to obtain a localized limited diffraction beam.

We first generalize a 3-D spherical wavelet solution developed by Kaiser *et al.* [24]–[26] to an n -dimensional space

$$\Phi_n(\vec{r}, t) = \frac{n(a_0 \pm ict)^2 - r^2}{[(a_0 \pm ict)^2 + r^2]^{\frac{n+3}{2}}}, \quad (7)$$

where $\Phi_n(\vec{r}, t)$ is a solution of (1) (see Appendix), $n \geq 1$ is an integer, $i = \sqrt{-1}$, a_0 is a constant, “ \pm ” represents that either the sign “+” or “-” is used in both the numerator and denominator of (7), and $r = \sqrt{\sum_{j=1}^n x_j^2}$. For $n = 3$ and $a_0 = 1$, we obtain Kaiser’s solution [26]

$$\Phi_3(\vec{r}, t) = \frac{3(1 - it')^2 - r^2}{[(1 - it')^2 + r^2]^3}, \quad (8)$$

where $\vec{r}' = (x, y, z)$ and $t' = ct$.

Notice that solution (7) specifies an n -dimensional localized wave. It appears in space-time for only a short duration and location and decays asymptotically in r and t directions in the power of $(n + 1)$. However, the peak (at $r \approx ct$ when $r \gg 1$) of the wave decays asymptotically in the power of $(n - 1)/2$ for $r \rightarrow \infty$. The importance of this solution is that the translates and dilates of (7) can be used as a basis to reconstruct the wave field at any $(x_1, x_2, \dots, x_n, t)$ from any source field [24]–[26].

From (7), we obtain the $(n - 1)$ -dimensional wavelet solution

$$\Phi_{n-1}(\vec{r}, t) = \frac{(n - 1)(a_0 \pm ict)^2 - r^2}{[(a_0 \pm ict)^2 + r^2]^{\frac{(n-1)+3}{2}}}, \quad (9)$$

where $r = \sqrt{\sum_{j=1}^{n-1} x_j^2}$. Using the variable substitution (3), we obtain an n -dimensional limited diffraction solution to (1)

$$\begin{aligned} \Phi_n(\vec{r}, t) &= \Phi_{n-1}(\vec{r}' \sin \zeta, x_n \cos \zeta / c - t) \\ &= \frac{(n - 1)(\alpha_0 \pm i(x_n \cos \zeta - ct))^2 - (r \sin \zeta)^2}{[(\alpha_0 \pm i(x_n \cos \zeta - ct))^2 + (r \sin \zeta)^2]^{\frac{(n-1)+3}{2}}}, \end{aligned} \quad (n - 1) \geq 1, \quad (10)$$

where $\vec{r}' = (x_1, x_2, \dots, x_{n-1})$ and $\vec{r} = (x_1, x_2, \dots, x_{n-1}, x_n)$. If $n = 3$, we have

$$\begin{aligned} \Phi_{2nd}(\vec{r}, t) &= \Phi_2(\vec{r}' \sin \zeta, z \cos \zeta / c - t) \\ &= \frac{2(\alpha_0 - i(z \cos \zeta - ct))^2 - (r \sin \zeta)^2}{[(\alpha_0 - i(z \cos \zeta - ct))^2 + (r \sin \zeta)^2]^{\frac{5}{2}}}, \end{aligned} \quad (11)$$

where the subscript “second” represents the second derivative of the zeroth-order X wave with respect to time (this will be explained in the next section), $x = x_1$, $y = x_2$, $z = x_3$, and “-” is chosen for (11) from “ \pm ” in (10). From the above example, we see that a localized wavelet wave (9) can be easily converted to a localized limited diffraction beam (10) or (11) by the variable substitution method developed in the last section. In the following, we will compare the limited diffraction beam obtained in (11) to other 3-D limited diffraction beams obtained previously.

IV. COMPARISON WITH OTHER LIMITED DIFFRACTION BEAMS

The limited diffraction solution (11) in the last section is called the second-derivative X wave because it is the second derivative of the zeroth-order X wave [15] with respect to time. This can be seen from its spectrum. Using the following Laplace transform pair [29],

$$\frac{\sqrt{\pi}}{\Gamma(\nu)} \left(\frac{k}{2\alpha} \right)^{\nu - \frac{1}{2}} J_{\nu - \frac{1}{2}}(\alpha k) \Leftrightarrow \frac{1}{(\tau^2 + a^2)^\nu}, \quad \text{for } \text{Re}(\nu) > 0, \quad (12)$$

where the Laplace transform is defined as

$$L(\tau) = \int_0^\infty f(k) e^{-\tau k} dk, \quad (13)$$

and assuming that $k = \omega/c$ is the wavenumber, $\alpha = r \sin \zeta$, and $\tau = a_0 - i(z \cos \zeta - ct)$, one can easily verify that the

Fourier transform of (11) gives

$$\begin{aligned} \tilde{\Phi}_{2\text{nd}}(\vec{r}, \omega) &= \frac{2\pi}{c} \left(\frac{\omega^2}{c^2} \right) \left[\frac{2}{\omega r \sin \zeta} J_1 \left(\frac{\omega}{c} r \sin \zeta \right) - J_2 \left(\frac{\omega}{c} r \sin \zeta \right) \right] \\ &\quad \times H \left(\frac{\omega}{c} \right) e^{-\frac{\omega}{c} (a_0 - iz \cos \zeta)} \\ &= \frac{2\pi}{c} \left(\frac{\omega}{c} \right)^2 J_0 \left(\frac{\omega}{c} r \sin \zeta \right) H \left(\frac{\omega}{c} \right) e^{-\frac{\omega}{c} (a_0 - iz \cos \zeta)}. \end{aligned} \quad (14)$$

In Eqs. (12) and (14), $J_m(\cdot)$ denotes the m th-order Bessel function of the first kind, $\Gamma(\cdot)$ is the Gamma function, and $H(\frac{\omega}{c})$ is defined as the following step function,

$$H \left(\frac{\omega}{c} \right) = \begin{cases} 1 & \text{for } \omega \geq 0 \\ 0 & \text{otherwise} \end{cases}, \quad (15)$$

and ω is the angular frequency. Compare (14) to the spectrum of the X waves obtained previously ((26) of [15]), it is seen that (14) is a special case for $n = 0$ and $B(\frac{\omega}{c}) = (\frac{\omega}{c})^2$ in [15]. From the properties of the Fourier transform, we know that (11) is proportional to the second derivative of (17) in [15] because multiplication of ω^2 in the Fourier domain is equal to the second-derivative in the time domain (see also (38) in [14]). Comparing (14) to the spectrum of a limited diffraction beam obtained by Donnelly *et al.* ((20) of [23]), we see that (11) is proportional to the first-derivative of that beam (see also (13) of [23] or (37) of [14]).

The properties of the second-derivative X wave (11) are shown in Fig. 1. For comparison, the first-derivative X wave ((13) of [23]) and the zero-th-order X wave ((17) of [15]) are also shown. The axial beam plots, spectra, lateral beam plots, and maximum sidelobes in lateral direction are given in Panels (1), (2), (3), and (4) of Fig. 1, respectively.

From (11) we see that the asymptotic decay of the field of the second-derivative X wave with the lateral distance r is of the order, $1/r^3$, at the axial distance $z = c_1 t$. This is similar to that of the limited diffraction beam obtained by Donnelly *et al.* [23] ($\sim 1/r^3$) and is different from the zeroth-order X wave [15] ($\sim 1/r$) (Panel (3) of Fig. 1). In addition, the spectrum of the second-derivative X wave is also similar to that of the first-derivative X wave [23]. It is a band-pass function and is different from that of the zeroth-order X wave (exponential function) (Panel (2) of Fig. 1). However, the maximum sidelobes of these limited diffraction beams remain about the same (Panel (4) of Fig. 1) and their asymptotic behavior is of the order $1/r^{1/2}$. Fortunately, several methods have been developed recently to reduce the sidelobes of limited diffraction beams [27], [28].

V. CONCLUSION

We have developed a novel approach that can convert any diffracting solution of the isotropic-homogeneous wave equation to a limited diffraction solution. As an example, the method was applied to a wavelet solution derived by Kaiser *et al.* [24]–[26] to obtain a localized limited diffraction beam that is called the second-derivative X wave because it is proportional to the second derivative of the zeroth-order X wave [15] (or the first derivative of the first-derivative X

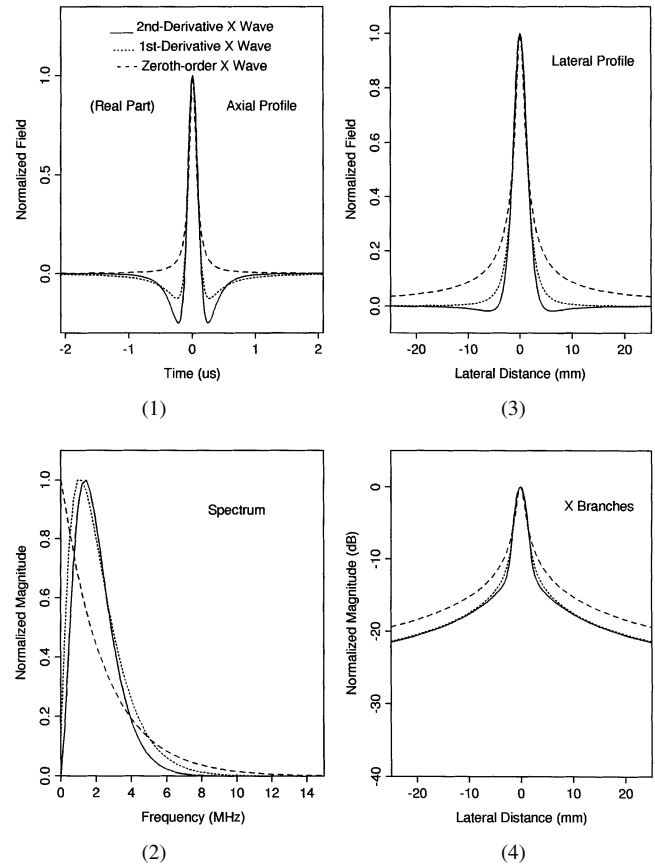


Fig. 1. Axial beam profiles of the second-derivative X wave (full lines), the first-derivative X wave (dotted lines) and the zeroth-order X wave (dashed lines) at $\vec{r} = 0$. (2) The spectra of (1). (3) The lateral, r , profiles of the beams at $z = c_1 t$, where $c_1 = c / \cos \zeta$ is the phase velocity of the waves. (4) The profiles of the waves along the X branches. The parameters used are as follows: $a_0 = 0.1$ mm, 0.22 mm, and 0.35 mm for the zeroth-order, the first-derivative, and the second-derivative X waves, respectively; the Axicon angle, ζ , is 6.6° ; and the real-part of the waves are used in the plots. Notice that the vertical scales are different in each panel.

wave [23]). This example establishes a relationship between localized limited diffraction beams and the wavelet waves. According to the simulation and experiment in [15] and [16], the second-derivative X wave can also be produced approximately with a practical ultrasonic transducer of finite aperture over a large depth of field (having an almost constant lateral and axial resolutions in the depth of field).

APPENDIX

Prove (7) is a solution to (1).

Proof: assume that

$$A = (a_0 \pm ict)^2 + r^2, \quad (A1)$$

and

$$T = n(a_0 \pm ict)^2 - r^2, \quad (A2)$$

then (7) is given by

$$\Phi_n(\vec{r}, t) = \frac{T}{A^{\frac{n+3}{2}}}, \quad (n \geq 1). \quad (A3)$$

It is easy to show that

$$\sum_{j=1}^n \frac{\partial^2 \Phi_n(\vec{r}, t)}{\partial x_j^2} = -\frac{2n}{A^{\frac{n+3}{2}}} + \frac{4(n+3)r^2 - n(n+3)T}{A^{\frac{n+5}{2}}} + \frac{(n+3)(n+5)r^2 T}{A^{\frac{n+7}{2}}} \quad (\text{A4})$$

and

$$\begin{aligned} & -\frac{1}{c^2} \frac{\partial^2 \Phi_n(\vec{r}, t)}{\partial t^2} \\ &= \frac{2n}{A^{\frac{n+3}{2}}} + \frac{-4n(n+3)(a_0 \pm ict)^2 - (n+3)T}{A^{\frac{n+5}{2}}} \\ &+ \frac{(n+3)(n+5)(a_0 \pm ict)^2 T}{A^{\frac{n+7}{2}}}. \end{aligned} \quad (\text{A5})$$

Therefore,

$$\begin{aligned} & \left[\sum_{j=1}^n \frac{\partial^2}{\partial x_j^2} - \frac{1}{c^2} \frac{\partial^2}{\partial t^2} \right] \Phi_n(\vec{r}, t) \\ &= -\frac{(n+3)(n+5)T}{A^{\frac{n+5}{2}}} + \frac{(n+3)(n+5)T}{A^{\frac{n+5}{2}}} \equiv 0. \end{aligned} \quad (\text{A6})$$

Proved.

ACKNOWLEDGMENT

The authors thank E. C. Quarve for secretarial assistance.

REFERENCES

- [1] J. N. Brittingham, "Focus wave modes in homogeneous Maxwell's equations: transverse electric mode," *J. Appl. Phys.*, vol. 54, no. 3, pp. 1179–1189, 1983.
- [2] R. W. Ziolkowski, "Exact solutions of the wave equation with complex source locations," *J. Math. Phys.*, vol. 26, no. 4, pp. 861–863, Apr., 1985.
- [3] R. W. Ziolkowski, D. K. Lewis, and B. D. Cook, "Evidence of localized wave transmission," *Phys. Rev. Lett.*, vol. 62, no. 2, pp. 147–150, Jan. 9, 1989.
- [4] A. M. Shaarawi, I. M. Besieris, and R. W. Ziolkowski, "Localized energy pulse train launched from an open, semi-infinite, circular waveguide," *J. Appl. Phys.*, vol. 65, no. 2, pp. 805–813, 1989.
- [5] I. M. Besieris, A. M. Shaarawi, and R. W. Ziolkowski, "A bidirectional traveling plane wave representation of exact solutions of the scalar wave equation," *J. Math. Phys.*, vol. 30, no. 6, pp. 1254–1269, 1989.
- [6] E. Heyman, B. Z. Steinberg, and L. B. Felsen, "Spectral analysis of focus wave modes," *J. Opt. Soc. Amer. A*, vol. 4, no. 11, pp. 2081–2091, Nov. 1987.
- [7] R. W. Ziolkowski, "Localized transmission of electromagnetic energy," *Phys. Rev. A*, vol. 39, no. 4, pp. 2005–2033, Feb. 15, 1989.
- [8] J. V. Candy, R. W. Ziolkowski, and D. K. Lewis, "Transient waves: reconstruction and processing," *J. Acoust. Soc. Amer.*, vol. 88, no. 5, pp. 2248–2258, Nov. 1990.
- [9] ———, "Transient wave estimation: a multichannel deconvolution application," *J. Acoust. Soc. Amer.*, vol. 88, no. 5, pp. 2235–2247, Nov. 1990.
- [10] R. W. Ziolkowski and D. K. Lewis, "Verification of the localized wave transmission effect," *J. Appl. Phys.*, vol. 68, no. 12, pp. 6083–6086, Dec. 15, 1990.
- [11] R. Donnelly and R. W. Ziolkowski, "Designing localized waves," *Proc. Royal Soc. Lond., A*, vol. 440, pp. 541–565, 1993.
- [12] J. Durnin, "Exact solutions for nondiffracting beams. I. The scalar theory," *J. Opt. Soc. Amer. A*, vol. 4, no. 4, pp. 651–654, 1987.
- [13] J. Durnin, J. J. Miceli Jr., and J. H. Eberly, "Diffraction-free beams," *Phys. Rev. Lett.*, vol. 58, no. 15, pp. 1499–1501, Apr. 13, 1987.
- [14] J. Lu, H. Zou, and J. F. Greenleaf, "Biomedical ultrasound beam forming," *Ultrasound Med. Biol.*, vol. 20, no. 5, pp. 403–428, July 1994.
- [15] J. Lu and J. F. Greenleaf, "Nondiffracting X waves—exact solutions to free-space scalar wave equation and their finite aperture realizations," *IEEE Trans. Ultrason., Ferroelec., Freq. Contr.*, vol. 39, pp. 19–31, Jan. 1992.
- [16] ———, "Experimental verification of nondiffracting X waves," *IEEE Trans. Ultrason., Ferroelec., Freq. Contr.*, vol. 39, pp. 441–446, May 1992.
- [17] ———, "Ultrasonic nondiffracting transducer for medical imaging," *IEEE Trans. Ultrason., Ferroelec., Freq. Contr.*, vol. 37, pp. 438–447, Sept. 1990.
- [18] ———, "Pulse-echo imaging using a nondiffracting beam transducer," *Ultrasound Med. Biol.*, vol. 17, no. 3, pp. 265–281, May 1991.
- [19] J. Lu, T. K. Song, R. R. Kinnick, and J. F. Greenleaf, "In vitro and in vivo real-time imaging with ultrasonic limited diffraction beams," *IEEE Trans. Med. Imag.*, vol. 12, no. 4, pp. 819–829, Dec. 1993.
- [20] J. Lu and J. F. Greenleaf, "Evaluation of a nondiffracting transducer for tissue characterization," *IEEE 1990 Ultrason. Symp. Proc.*, 90CH2938–9, vol. 2, pp. 795–798, 1990.
- [21] ———, "Producing deep depth of field and depth-independent resolution in NDE with limited diffraction beams," *Ultrason. Imag.*, vol. 15, no. 2, pp. 134–149, Apr. 1993.
- [22] ———, "Application of Bessel beam for Doppler velocity estimation," *IEEE Trans. Ultrason., Ferroelec., Freq. Contr.* vol. 42, no. 4, pp. 649–662, July 1995.
- [23] R. Donnelly, D. Power, G. Templeman, and A. Whalen, "Graphic simulation of superluminal acoustic localized wave pulses" *IEEE Trans. Ultrason., Ferroelec., Freq. Contr.*, vol. 41, no. 1, pp. 7–12, 1994.
- [24] G. Kaiser, "Wavelet electrodynamics," *Phys. Lett. A*, vol. 168, pp. 28–34, 1992.
- [25] ———, "Space-time-scale analysis of electromagnetic waves," *Proc. IEEE-SP Inter. Symp. Time-Frequency and Time-Scale Analysis*, 1992.
- [26] G. Kaiser and R. F. Streater, "Windowed radon transforms, analytic signals and the wave equation," *Wavelets—A Tutorial in Theory and Applications*, C. K. Chui, Ed. New York: Academic, 1992.
- [27] J. Lu and J. F. Greenleaf, "Sidelobe reduction for limited diffraction pulse-echo systems," *IEEE Trans. Ultrason., Ferroelec., Freq. Contr.*, vol. 40, no. 6, pp. 735–746, Nov. 1993.
- [28] J. Lu, "Bowtie limited diffraction beams for low sidelobe and large depth of field imaging," *IEEE Trans. Ultrason., Ferroelec., Freq. Contr.*, to be published.
- [29] I. S. Gradshteyn and I. M. Ryzhik, *Tables, Integrals, Series, and Products*. San Diego, CA: Academic, 1980.

Jian-yu Lu (M'88) for a photograph and biography see p. 661 of the July 1995 issue of this TRANSACTIONS.

Hehong Zou, for a photograph and biography see p. 662 of the July 1995 issue of this TRANSACTIONS.

James F. Greenleaf (M'73–SM'84–F'88) for a photograph and biography see p. 662 of the July 1995 issue of this TRANSACTIONS.